

# Adsorptive Removal of Cd(II) Ions Using Zinc oxide and Iron doped zinc oxide nanoparticles

Amita Khatri<sup>1</sup>, Parul Yadav<sup>2</sup>, Anu Kumari<sup>1</sup>, Meenu Yadav<sup>1</sup>, Rachna Bhateria<sup>1\*</sup>

<sup>1</sup>Department of Environmental Science, Maharshi Dayanand University, Rohtak- 124001, Haryana, India

<sup>2</sup>Department of Chemistry, Indian Institute of Technology Roorkee, Roorkee- 247667, Uttarakhand, India

\*Corresponding author: email: [rachna.env@mdurohtak.ac.in](mailto:rachna.env@mdurohtak.ac.in)

## Abstract

The nanoparticles were synthesized through the chemical co-precipitation method. Zeta potential analysis and scanning electron microscopy (SEM) were utilized to characterize the surface properties, stability, and morphology of the Zinc oxide nanoparticles (ZnO NPs) and iron-doped zinc oxide nanoparticles (Fe-ZnO NPs). ZnO NPs and Fe-ZnO NPs were investigated for the adsorption of Cd(II) ions under different operating conditions, including pH, adsorbent dosage, contact time, initial metal ion concentration, and temperature. Adsorption efficiency increased with increasing pH and reached optimum values at pH 6 for Fe-ZnO NPs and pH 7 for ZnO NPs, whereas further increase in pH reduced adsorption due to the precipitation of Cd(OH)<sub>2</sub>. Compared with ZnO NPs, Fe-ZnO NPs exhibited enhanced adsorption performance, which can be attributed to their improved surface properties and higher affinity toward Cd(II) ions. Adsorption efficiency increased with increasing adsorbent dosage and contact time until equilibrium was attained. Although higher initial Cd(II) concentrations enhanced the adsorption capacity, the percentage removal decreased due to saturation of the available active sites. Temperature studies revealed that adsorption performance improved up to 35–40 °C, after which a decline was observed at elevated temperatures. Overall, Fe-ZnO NPs exhibited superior Cd(II) removal efficiency compared to ZnO NPs, highlighting their potential as effective nanoadsorbents for wastewater remediation applications.

**Keywords:** nanoparticles, ZnO NPs, Fe-ZnO NPs, heavy metal, cadmium(II) ions, optimization

**How to cite this article:** Khatri A, Yadav P, Kumari A, Yadav M, Bhateria R. Adsorptive Removal of Cd(II) Ions Using Zinc oxide and Iron doped zinc oxide nanoparticles. *Int J Drug Deliv Technol.* 2026;16(56s): 703-708. DOI: 10.25258/ijddt.16.56s.74

## INTRODUCTION

Owing to their high solubility and non-biodegradable nature, toxic metals are difficult to remove using conventional treatment methods and often cause secondary pollution, rendering treated water unsuitable for human and animal use. As a result, the generation of metal-laden wastewater contributes to water scarcity, increased treatment costs, and limited access to clean water in affected communities. Persistent, toxic, and non-biodegradable heavy metals in water pose serious risks to humans and the environment. Even at low concentration, metals like Cr, Pb, Cd, Ni, Hg, and Co can cause severe health issues, including organ damage, neurological disorders, and even death.<sup>1</sup>

Nano-based adsorbents, particularly those derived from low-cost materials, have gained significant attention for the removal of heavy metals from water. Their high surface area and abundant functional groups provide numerous active sites for enhancing adsorption efficiency. As a result, nanoparticles exhibit superior metal removal performance through various physicochemical interactions. Heavy metal ions such as Cd<sup>2+</sup>, Pb<sup>2+</sup>, Cr<sup>2+</sup>, and Hg<sup>2+</sup> ions interact with nanoparticle surfaces through mechanisms like electrostatic attraction, surface complexation, ion

exchange, chelation, and redox reactions. The efficiency of these interaction depends on the nanoparticles' functional groups, surface charge, and the solution pH. In metal oxide nanoparticles (e.g., ZnO, Fe<sub>3</sub>O<sub>4</sub>, TiO<sub>2</sub>), surface hydroxyl (–OH) groups play a crucial role by forming inner-sphere or outer-sphere complexes with metal ions, leading to strong and often irreversible adsorption.<sup>2</sup>

In doped or composite nanoparticles, lattice defects and heterogeneous surfaces increase the number of active binding sites, enhancing metal adsorption. Carbon-based and functionalized nanomaterials further interact with heavy metals via  $\pi$ -electron interactions and coordination with oxygen-, nitrogen-, or sulfur-containing groups. Overall, their strong affinity, fast kinetics, and tunable surface properties make nanoparticles highly effective for water and wastewater treatment. <sup>3</sup>ZnONPs with their high surface area and abundant surface hydroxyl groups, enable strong electrostatic interactions and surface complexation with Cd(II) ions.

The introduction of iron into the lattice of ZnO NPs boosts adsorption performance by enhancing surface heterogeneity, generating additional active sites, and increasing structural defects, all of which contribute to stronger metal-adsorbent interactions. This is due to

\*Author for Correspondence: [rachna.env@mdurohtak.ac.in](mailto:rachna.env@mdurohtak.ac.in)

the synergistic effects between ZnO NPs and iron species, as well as improved charge transfer and enhanced surface reactivity.<sup>4</sup>

In this study, zinc oxide and iron-doped zinc oxide nanoparticles were synthesized and applied for the removal of Cd(II) ions from aqueous solution. The adsorption behavior was systematically evaluated using isotherm, kinetic and thermodynamic analysis.

## MATERIALS AND METHODS

### Reagents and Equipment

All reagents used were of analytical grade. A 1000 mg/L Cd(II) stock solution was prepared and diluted with deionized water to obtain working solutions. The pH was adjusted using 1 N H<sub>2</sub>SO<sub>4</sub> or 1 N NaOH and measured with a digital pH meter. Residual Cd(II) concentration was determined using an Atomic Absorption Spectrophotometer (AAS).

### Preparation of adsorbents

A 1 M NaOH solution was prepared using distilled water and heated to 50–90 °C with continuous stirring. A 0.5 M ZnCl<sub>2</sub> solution was then added dropwise, resulting in the immediate formation of a white ZnO precipitates. The mixture was stirred for 2 hours, after which the precipitate was separated and thoroughly washed with distilled water to remove residual NaCl. The product was further processed by centrifugation, ultrasonication, and dispersion in 2-propanol, followed by drying in a vacuum oven at temperatures below 70 °C.<sup>5</sup>

The precipitation method offers a simple and cost-effective route for nanoparticle synthesis. Zinc acetate dihydrate and FeCl<sub>3</sub> were dissolved in deionized water and ethanol to form solution A, while solution B (1 M NaOH) was added gradually to induce precipitation. The precipitate was aged for two days, then filtered, dried at 70 °C, and finally calcined at 300 °C for 30 hours.<sup>6</sup>

### Characterization of Adsorbents

The particle size distribution of the synthesized nanoparticles were determined using a zeta sizer (Zets Sizer, Malvern nano zs). Scanning electron microscopy (SEM) was used for surface morphology of the ZnO NPs and Fe–ZnO NPs (Zeiss Gemini 560, IIT, Roorkee).

### Batch Experiments

All experiments were conducted in batch mode to evaluate the effects of pH, adsorbent dosage, contact time, initial concentration, and temperature on adsorption performance of nanoparticles. The experiments were carried out using 100 mL of Cd(II) solutions with varying initial concentrations (10–100

mg L<sup>-1</sup>), indicating efficient Cd(II) uptake by nanoparticles at higher concentrations. Adsorbent doses ranging from 20 mg – 160 mg were studied at a constant agitation speed of 200 rpm over a pH range of 1–10. Experiments for optimizing contact time were conducted for durations of 20 –180 min, while temperature effects were examined between 10 and 55 °C. The solution pH was adjusted using 0.1 M HCl and 0.1 M NaOH. All experiments were performed in triplicate, and average values were used for analysis. The equilibrium Cd(II) concentration was first determined using an atomic absorption spectrophotometer (AAS). Based on this, the equilibrium adsorption capacity ( $q_e$ , mg g<sup>-1</sup>) was calculated from the amount of metal adsorbed per unit mass of adsorbent.

$$\text{Uptake capacity } (q_e) = \frac{C_i - C_e}{m} \times V \quad (1)$$

$$\text{Removal efficiency } (\%) = \frac{C_i - C_e}{C_i} \times 100 \quad (2)$$

The equilibrium adsorption capacity ( $q_e$ , mg g<sup>-1</sup>) was calculated using Eq. (1) as the amount of Cd(II) adsorbed per unit mass of adsorbent, where V is the solution volume (L), x is the adsorbent mass (g), and C<sub>i</sub> and C<sub>e</sub> are the initial and equilibrium Cd(II) concentrations (mg/L), respectively. The percentage removal of Cd(II) by ZnO NPs and Fe–ZnO NPs was determined using Eq. (2), based on the values of C<sub>i</sub> and C<sub>e</sub>.

## RESULTS AND DISCUSSION

### Zeta size distribution

The observed particle size below 100 nm confirms the nanoscale nature of the synthesized material, which is favorable for enhanced adsorption efficiency. Nanoparticles in the 1–100 nm range exhibit unique physicochemical properties and improved interaction with contaminants.<sup>7</sup> The particle size distribution profile is shown in Fig. 1. which provide insight into the hydrodynamic size and dispersion behavior of ZnO NPs and Fe–ZnO NPs in suspension. In Figure 1 (a), the ZnO NPs exhibit a relatively sharp and narrow peak centered at a higher particle size range, indicating the presence of larger hydrodynamic diameters. These results suggested that ZnO NPs tend to aggregate in aqueous media, likely due to their high surface energy and strong interparticle interactions whereas Fe–ZnO NPs shown in Fig. 1. (b) displayed a shift toward smaller particle sizes with a narrower and more uniform distribution. This indicates that iron doping enhances dispersion and reduces aggregation.

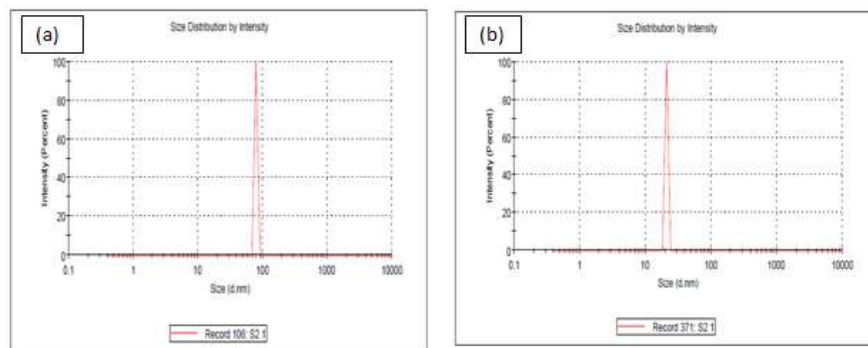


**Figure 1:** Zeta size distribution (a) ZnO NPs, (b) Fe-ZnO NPs

### SEM Analysis

FESEM (Fig.2) illustrated the surface morphology of the synthesized nanoparticles. Figure. 2. (a) corresponding to ZnO NPs revealed irregular, flake- and plate-like structures that are densely packed with pronounced agglomeration. The particles appeared fused into larger clusters, resulting in a broad and non-uniform size distribution. Such agglomeration is typically associated with the high surface energy and strong interparticle forces of ZnO NPs, which reduced the effective surface area and limited the accessibility of active adsorption sites.<sup>8</sup> Consequently, ZnO NPs exhibited comparatively lower adsorption performance due to the reduced number of available sites for interaction with metal ions. In contrast, Fig. 2. (b) of Fe-ZnO NPs showed a significant modification in morphology as a result of iron doping. Compared to ZnO NPs the particles seemed smaller, more evenly distributed, and less clustered. The surface exhibits a structure that is relatively porous and loosely packed, increasing the exposure of active sites.

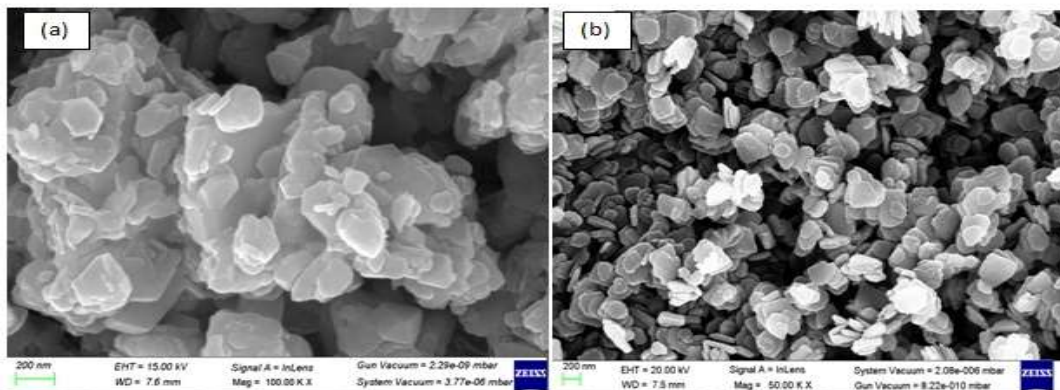


**Figure 2:** Surface Morphology of (a) ZnO NPs and (b) Fe-ZnO NPs

### Effect of various parameters

The adsorption performance of Cd(II) ions using ZnO NPs and Fe-ZnO NPs was systematically evaluated under different experimental conditions to investigate their removal efficiency and adsorption behavior. Important operational parameters, including pH, adsorbent dosage, contact time, initial metal ion concentration, and temperature, were optimized to determine the most favorable conditions for effective Cd(II) adsorption (Figure 3).

### Effect of pH

Solution pH is a key controlling parameter in adsorption processes that significantly influenced the removal of Cd(II). Adsorption efficiency increased from pH 2 to 4, remained nearly constant up to pH 5, and rose again, reaching a maximum around pH 6 for Fe-ZnO NPs and pH 7 for ZnO NPs. At low pH, adsorption was limited due to competition from H<sup>+</sup>

ions and electrostatic repulsion. With increasing pH, adsorption improved owing to favorable electrostatic interactions, but declined beyond the optimum range due to metal hydroxide formation. Fe-ZnO NPs exhibited superior performance, indicating enhanced surface properties and adsorption affinity due to iron doping. At pH values above 7, Cd(II) removal decreased primarily due to the formation of Cd(OH)<sub>2</sub> precipitates, which reduced the availability of free Cd(II) ions for adsorption.<sup>9</sup> Although anionic cadmium complexes may form, their contribution is minimal due to weaker interactions with the adsorbent.<sup>10</sup> Thus, the decline in adsorption at higher pH is mainly governed by changes in metal speciation and precipitation rather than electrostatic effects.

### Effect of adsorbent dose

Cd(II) adsorption increased with adsorbent dose due to the availability of more active sites, reaching an

optimum at 60 mg for Fe–ZnO NPs and 100 mg for ZnO NPs. Beyond this, only marginal or reduced efficiency was observed due to nanoparticle aggregation and overlap of active sites, which lowered the effective surface area.<sup>11</sup> Fe–ZnO NPs exhibited superior performance, achieving higher Cd(II) removal at lower dosages compared to ZnO NPs. Increasing adsorbent dose enhanced removal efficiency due to more available active sites, however, beyond the optimum level, adsorption capacity decreased due to particle aggregation and overlap of adsorption sites.<sup>12, 13</sup>

**Effect of Contact time**

Cd(II) removal increased rapidly at initial contact due to abundant active sites, then slowed and reached equilibrium as sites became saturated and intraparticle diffusion resistance increased.<sup>14</sup> ZnO NPs attained maximum adsorption at 60 min, followed by a slight decline, indicating possible desorption. In contrast, Fe–ZnO NPs showed a gradual increase, reaching stable equilibrium around 100 min with better overall performance. The enhanced adsorption of Fe-ZnO NPs is attributed to improved surface properties and stronger adsorbent–adsorbate interactions due to iron doping. Cd(II) removal increased rapidly initially due to abundant active sites, then becomes diffusion-controlled and reached equilibrium with minimal further change.

**Effect of initial metal ion concentration**

Adsorption performance is strongly affected by the initial Cd(II) concentration. The adsorption capacity ( $q_e$ ) increased with concentration due to a higher mass transfer driving force, while percentage removal decreases at higher concentration because of site saturation.<sup>15</sup> Fe–ZnO NPs exhibited superior adsorption compared to ZnO NPs. At higher Cd(II) concentrations, adsorption reached a plateau or slightly declines due to saturation of active sites. While adsorption capacity ( $q_e$ ) increases with concentration because of a greater mass transfer driving force, percentage removal decreases due to site saturation and increased ion competition.<sup>16</sup>

**Effect of Temperature**

The increase in adsorption capacity with temperature indicated an endothermic process, likely due to enhanced Cd(II) mobility and greater availability of active sites. Adsorption efficiency for both ZnO NPs and Fe–ZnO NPs improved up to 35–40 °C, reflecting better diffusion and site activation, but declined at higher temperatures due to weakened interactions and increased desorption. Fe–ZnO NPs showed superior thermal stability and adsorption performance, highlighting the beneficial effect of iron doping. Temperature played a crucial role in Cd(II) adsorption using nanoparticles. The decrease in adsorption capacity with increasing temperature indicated an exothermic process, as high temperature weakens the adsorbent–adsorbate interaction.<sup>17</sup> However, elevated temperatures can enhance adsorption kinetics by improving diffusion and mass transfer.

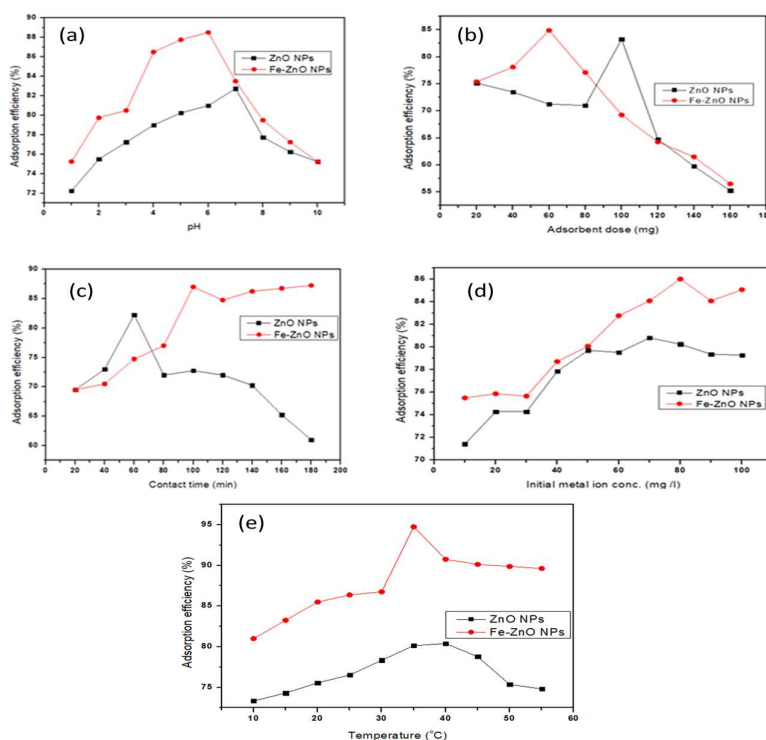


**Figure 3:** Influence of (a) pH, (b) adsorbent dose, (c) contact time, (d) initial Cd(II) conc., (e) temperature on Cd(II) adsorption using ZnO NPs and Fe-ZnO NPs

## CONCLUSION

The study demonstrated that both ZnO NPs and Fe-ZnO NPs were effective in removing Cd(II) ions from aqueous solutions, with Fe-ZnO NPs exhibiting comparatively higher adsorption efficiency. The adsorption process was strongly influenced by factors such as pH, adsorbent dosage, contact time, initial Cd(II) concentration, and temperature. Maximum adsorption was achieved under near-neutral pH conditions, moderate adsorbent dosage, and sufficient equilibrium time. Iron incorporation significantly enhanced the surface characteristics, stability, and adsorption affinity of ZnO nanoparticles, resulting in improved Cd(II) removal even at lower dosages. These findings indicate that Fe-ZnO NPs are promising and sustainable adsorbents for efficient cadmium remediation from wastewater systems.

**Conflict of Interest :** The author declare no conflict of interest.

## 2) Acknowledgements

**Life Science Reporting:** No life science threat was practiced in this research.

**Funding Information:** No funding was received for this research.

## 3) Author's Contribution

Amita Khatri: Experiment performing, writing original draft,

Parul Yadav : Methodology, Validation, Draft editing;

Anu Kumari: Methodology, and Draft editing;

Meenu Yadav: Methodology and Draft editing;

Rachna Bhateria : Conceptualization, Editing and Reviewing, ResearchGuidence

**Declaration of interests:** The authors declare that they have no known competing financial interests or personal relationships that could have appeared to influence the work reported in this paper.

## REFERENCES

- Dhiman V, Kondal N. ZnONanoadsorbents: A potent material for removal of heavy metal ions from wastewater. *Colloid and Interface Science Communications*. 2021 1;41:100380.
- Motitswe MG, Badmus KO, Khotseng L. Application of reduced graphene oxide-zinc oxide nanocomposite in the removal of Pb (II) and Cd (II) contaminated wastewater. *Applied Nano*. 2024 9;5(3):162-89.
- Feisal NA, Kamaludin NH, Ahmad MA, Ibrahim TN. A comprehensive review of nanomaterials for efficient heavy metal ions removal in water treatment. *Journal of Water Process Engineering*. 2024 Jul 1;64:105566.
- Singh K, Lohchab RK, Goel G, Waziri SA, Aguedal H, Allab Y, Elmeliani ME, Iddou A, Liu B, Terashima M, Kaswan S. Innovative use of immobilized zinc oxide-impregnated activated carbon (ZnO@ CB) for effective treatment of leachate: modeling and predictive assessment. *Environmental Science and Pollution Research*. 2025;32(23):13803-19.
- Divya B, Karthikeyan CH, Rajasimman M. Chemical synthesis of zinc oxide nanoparticles and its application of dye decolourization. *International Journal of Nanoscience and Nanotechnology*. 2018;14(4):267-75.
- Paganini MC, Giorgini A, Gonçalves NP, Gionco C, Prevot AB, Calza P. New insight into zinc oxide doped with iron and its exploitation to pollutants abatement. *Catalysis Today*. 2019; 15;328:230-4.
- Ethaib S, Al-Qutaifia S, Al-Ansari N, Zubaidi SL. Function of nanomaterials in removing heavy metals for water and wastewater remediation: A review. *Environments*. 2022 25;9(10):123.
- Umar RD, Titus I, Joseph E, Mamman UG. Molecular characterization of multidrug resistance genes and effect of zinc oxide nanoparticles on *Salmonella typhi* serovars from clinical specimens. *Journal of Advances in Microbiology Research*. 2025;6(2):100-5.
- Pang Y, Wen J, Liu H, Xu Z, Yu F, Wang J, Huang G, Xu S. Selective platinum recovery from Pt-Co solutions via amine/phosphine oxide-loaded solvent-impregnated resins: mechanisms and selectivity. *Journal of Cleaner Production*. 2025; 1;526:146627.
- Mubarak MF, Yousef TA, Salim SA, Khairy M, Kamoun EA, Mahmoud T. Meta-kaolinite metal oxide quaternary composite for layered double hydroxide applied to a new frontier in adsorption technology: Synthesis, adsorption performance and kinetics study. *Inorganic Chemistry Communications*. 2025; 178:114647.
- Chen B, Li C, Song J, Dai X, Lu Z, Zhou Z, Wang Q, Dai L. Removal of Cl-from contaminated acid by resin adsorption: Kinetics, isothermal model, approximate site energy distribution and adsorption mechanism. *Journal of Environmental Chemical Engineering*. 2025;13(3):116656.
- Datta J, Deb S. Tea factory waste as a cost-effective and sustainable cadmium (II) adsorbent: Investigating adsorption isotherms, kinetics, and thermodynamics. *Physics and Chemistry of the Earth, Parts A/B/C*. 2025; 29:104042.
- Gürsoy S, Zeytinci NK, Zaman BT, Bakırdere S, Öztürk Er E. Study of linear and nonlinear isotherm and kinetic parameters of hexavalent chromium adsorption onto reduced graphene oxide coated iron oxide. *Scientific Reports*. 2025 ;15(1):25206.
- Khan MS, Khalid M, Shahid M. What triggers dye adsorption by metal organic frameworks? The current perspectives. *Materials Advances*. 2020;1(6):1575-601.
- Mahmoud EN, Fayed FY, Ibrahim KM, Jaafreh S. Removal of cadmium, copper, and lead from water using bio-sorbent from treated olive mill solid residue. *Environmental Health Insights*. 2021 ;15:11786302211053176.
- Toussi AG, Einafshar E, Rafati SS. Potential of Graphene Nanoparticles for Reducing Cadmium

- Toxicity and Environmental Contamination.  
Journal of Toxicology. 2026;2026(1):7838711.
17. Obaid ZH, Salman JM, Ali SS, Abdul-Adel E, Juda SA. Utilization of Immobilized Green Algae *Scenedesmus quadricauda* as A Sustainable Method to Remove Some Industrial Textile Dyes. Diyala Agricultural Sciences Journal. 2025 Jun 30;17(1):30-45.